Робота присвячена розробці і випробуванню електрохромного пристрою на основі композитної плівки $Ni(OH)_2$/ПВС (полівінілового спирту) і сітчастого протиелектрода. У якості матеріалу сітчастого електрода був використаний мідний дріт з гальванічно нанесеним срібним покриттям. В якості основи для осадження електрохромного матеріалу було використано скло з покриттям, яке складалось з оксида олова, допованого фтором, який піддавали спеціальній обробці. Обробка полягала в неглибокому розчиненні поверхні методом м'якого електрохімічного травлення. Відстань поміж сітчастим та електрохромним електродами була невеликою і складала 1,5 мм.

Запропонована конструкція електрохромного пристрою може привести до значного зменшення його собівартості. З іншого боку заявлена конструкція накладає обмеження на спектр можливого її застосування: верхні частини оглядових вікон, світлові вікна, перегородки в приміщеннях.

В результаті проведення досліджень було показано, що електрохромний пристрій працездатний і може бути використаний як прототип для подальшого масштабування. Також в результаті випробувань були підібрані параметри електрохімічного циклування – вікно робочих напруг і робоча густина струму. Встановлено, що використання гальваностатичного режиму при затемненні та освітленні приводить до лінійних оптичних характеристик пристрою. Використання обраного вольтдинамічного режиму веде до погіршення питомих характеристик пристрою – глибини затемнення і оберненості при освітленні.

Показано, що у результаті близькості робочих потенціалів оксиднонікелевого і срібного електродів при затемненні і освітленні напруга пристрою змінює полярність. Крім того, було відзначено, що протягом усіх експериментів газовиділення на електродах пристрою не спостерігалось

Ключові слова: гідроксид нікелю, полівініловий спирт, електрохромний пристрій, сітчастий електрод, травлення, протиелектрод, срібло

UDC 544.653.1
DOI: 10.15587/1729-4061.2019.181396

A STUDY OF AN ELECTROCHROMIC DEVICE BASED ON $NI(OH)_2$/PVA FILM WITH THE MESH-LIKE SILVER COUNTER ELECTRODE

V. Kotok
PhD, Associate Professor
Department of Processes, Apparatus and General Chemical Technology*
E-mail: valeriykotok@gmail.com
Senior Researcher**
V. Kovalenko
PhD, Associate Professor
Department of Analytical Chemistry and Food Additives and Cosmetics*
E-mail: vadimchem@gmail.com
Senior Researcher**
*Ukrainian State University of Chemical Technology
Gagarina ave., 8, Dnipro, Ukraine, 49005
**Competence center "Ecological technologies and systems"
Vyatka State University
Moskovskaya str., 36, Kirov, Russian Federation, 610000

Received date 17.06.2019
Accepted date 02.10.2019
Published date 31.10.2019

1. Introduction

"Smart" devices are more often being developed and used for the optimization of power consumption, reducing the usage of resources and time requirements for various processes. It is expected that "smart" devices would become the basis for "smart" houses, which in turn would be elements of "smart" cities. The creation of "smart" cities would allow for advancement onto a new level of utilization of planet's limited resources.

"Smart" devices are most commonly devices that combine a conventional device and controller (a mini computer) that controls it. A device can be equipped with various sensors, interfaces and can be connected to the Internet. This allows for flexible control over the devices leading to rational resource utilization [1].

One of the promising developments are "smart" windows. These devices are able to switch the optical properties of transparent parts, such as color, glossiness, reflectivity. The use of such windows in different fields can improve comfort and significantly reduce the power consumption of a building. The power savings come from partially shaded windows blocking sunlight during periods of high solar radiation. The latter leads to the reduction in power consumption required for air conditioning [2, 3].

Despite significant advantages of this technology, the high cost, ranging within 100–400 USD/m^2 [4, 5], limits its widespread use. Thus, the search for cheaper technologies for manufacturing electrochromic devices is a relevant scientific problem [6].

2. Literature review and problem statement

The primary goal for widespread adoption of this technology is lower cost of assembled finished devices. It is known that there are two main reasons for the high cost of electrochromic devices. First – small production volume, which leads to the distribution of expenses onto small batches of produced "smart" windows [7]. Second – relatively high cost of vacuum methods of film deposition used to form layers of the device [8, 9].

The design of electrochromic devices that is used presently is shown in Fig. 1, *a*. The design consists of two electrochromic materials (cathodic and anodic), two conductive transparent layers and electrolyte [10, 11]. There are two main implementations – completely solid-state and with thickened electrolyte. The completely solid-state device is manufactured through sequential sputtering of layers onto glass using separate apparatuses [12]. The second implementation lies in manufacturing two half-elements that consist of glass, conductive layer and electrochrome [13]. The half-elements are assembled with thickened electrolyte in-between. The electrolyte is usually based on a propylene carbonate solution of $LiClO_4$ [12, 13]. In both cases, there are 4–5 vacuum sputtered oxide layers. Despite the smaller number of layers, the thickened electrolyte variant requires expensive lithium salt and high purity propylene carbonate, which is also expensive.

The paper [14] proposes a modification of the existing design (Fig. 1, *b*) with the aim of cost reduction. The use of the mesh with electrochemically active material alleviates the need for two vacuum sputtered layers. This also allows for the use of materials active in aqueous electrolytes [14]. In theory, such design should be cheaper due to fewer sputtered layers and use of aqueous electrolyte.

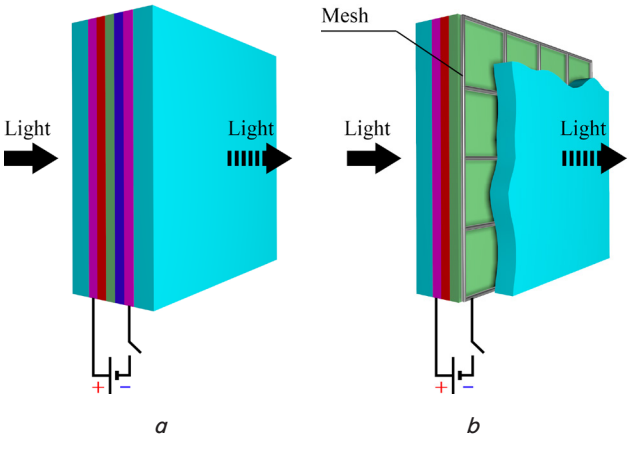

Fig. 1. Designs of electrochromic devices (— glass; — conductive transparent layer; — anodic electrochrome; — electrolyte; — cathodic electrochrome): *a* — conventional electrochromic device; *b* — electrochromic device with mesh counter-electrode

It should be noted that the obvious disadvantage of such design is the presence of opaque parts where mesh material is. Nevertheless, this isn't a limitation for light windows or upper parts of view windows.

A $Ni(OH)_2$-based film can be used as the main electrochromic electrode [15, 16]. It is worth saying that this material is also widely used in current sources [17]. Copper wire coated with silver can be used for manufacturing the mesh electrode [14].

A physical limitation for such design is the non-uniform coloration of electrochrome due to non-uniform current distribution [18]. The cause of the non-uniform current distribution in such design is a small distance between electrodes and geometric irregularity of the mesh.

Considering the probability of non-uniform current distribution [19, 20], during coloration (bleaching) there are three possible operation scenarios of such device:

– the assembled device is colored (bleached) uniformly – i. e. the entire electrode surface would have uniform color during its operation;

– the assembled device would change its color in regions near the conductor of the mesh electrode;

– the device would change color across its whole surface with regions of uneven coloration.

In case of the latter scenario, another question arises – is there a way to somehow reduce or eliminate color non-uniformity? Considering that such designs are currently not used for electrochromic devices and structural innovations are an important aspect, which is reviewed in the scientific literature [21], investigation of assumed scenarios is necessary.

The main problem of this study is to investigate how operational is such design of the electrochromic device with chosen materials of mesh and electrochromic electrodes.

It should also be mentioned that employed deposition methods and pre-treatment methods for electrode preparation are chosen based on previously found optimal conditions [16, 24, 25].

3. The aim and objectives of the study

The aim of the study is to evaluate the operation of the electrochromic device with mesh counter-electrode and $Ni(OH)_2$-based film with an aqueous electrolyte.

The evaluation is necessary to understand how uniform the coloration process would be with chosen geometrical parameters and materials.

To achieve the set aim, the following objectives were formulated:

– to assemble the electrochromic device with chosen materials: silver mesh electrode and electrochromic $Ni(OH)_2$/PVA;

– to conduct testing of the assembled device and evaluate its operability in aqueous electrolyte (0,1 KOH).

4. Materials and methods used for assembly and study of electrochromic device

Device assembly. To assemble the electrochromic device, an electrochromic electrode and counter-electrode modeling one cell of a 2×2 cm square mesh electrode were used. A copper wire with the electrodeposited layer of silver (commercial source) was used to construct the model mesh electrode. Wire diameter – 1 mm, coating thickness – 30 μm. Glass substrate with the layer of SnO_2:F (FTO glass, Zhuhai Kaivo Optoelectronic Technology Co., China) was used as the main (electrochromic) electrode. Sheet resistance of FTO glass ≈9 Ω/□.

The electrochromic device was assembled according to the scheme shown in Fig. 2.

In the first stage (1, Fig. 2), 3×2 cm FTO glass was washed with a soda solution and distilled water. Then it was treated in an ultrasonic bath (41.5 kHz, 60 W) for10 min, in ethanol to remove any contaminants. Then it was subjected to soft electrochemical etching [22] to form surface micro-roughness (2, Fig. 2). The method lies in partial dissolution of SnO_2:F surface with impulses of alternating electrical current in 1 M HCl. The use of this method allows improving the adhesion and working char-

acteristics of the deposited film [22]. After etching, the substrate was washed with distilled water and placed into a cell for the deposition of a composite $Ni(OH)_2$/PVA film (PVA – polyvinyl alcohol).

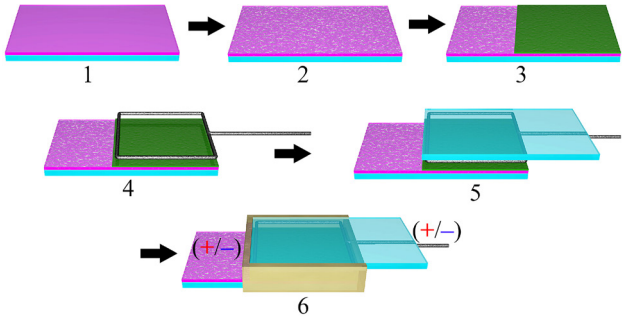

Fig. 2. Stages of electrochromic device assembly. Colors represent materials: — glass, —SnO_2:F, — composite $Ni(OH)_2$/PVA film, — silver-coated copper wire, — thermal adhesive (schematic representation): 1 — initial glass coated with SnO_2:F (FTO glass); 2 — soft etching of SnO_2:F coating [22]; 3 — electrochemical deposition of composite $Ni(OH)_2$/PVA film; 4, 5 — introduction of a square of silver-coated copper wire and glass; 6 — sealing of electrochromic device along the edges with thermal adhesive

The electrochromic film was deposited from a solution of 0.01 M $Ni(NO_3)_2$ with the addition of 4 % PVA (polyvinyl alcohol) at a cathodic current density of 0.1 mA/cm^2 for 10 min [17, 23, 25]. Working electrode area 2×2 cm (3, Fig. 2). Nickel foil was used as a counter-electrode.

Silver-coated copper wire was bent into a 2×2 cm square and cycled in 0.1 M base solution as a surface treatment: potential window –599–+1,001 mV (NHE), 10 mV/s, 5 cycles.

At the end of cycling, the electrode potential was swept from 201 to 1,001 mV (NHE) at 10 mV/s and stopped. The last step was made to form oxidized silver species – Ag_XO_Y. The obtained mesh electrode, along with a regular glass (3×2 cm, without SnO_2:F) was used to assemble the electrochromic device (4 and 5, Fig. 2). The distance between the mesh electrode and glass with the electrochromic film was set to about1.5 mm. The device was then sealed along edges with thermal adhesive (6, Fig. 2). After the adhesive has cured, the space inside the cell was filled with electrolyte – 0.1 M KOH (6, Fig. 2) using a syringe. The hole left from siring was then sealed with thermal adhesive (Akfix HM-208, based on ethylenevinylacetate).

Characterization of electrochromic device. Electrochemical cycling was conducted using a digital potentiostat (Elins, P-8, Russia) in different regimes in a two-electrode configuration. Optical properties were recorded in parallel with electrochemical cycling. The device used to record the optical characteristics is shown in Fig. 3.

In this setup, an E-154 analog-to-digital converter (Russia) was used along with software distributed with it.

A separate electrochromic electrode was prepared in the same way to determine the working current. The electrode was then cycled in a cell with free electrolyte volume, between 201–751 mV (NHE) at a scan rate of 1 mV/s [23]. Nickel foil was used as a counter-electrode, reference electrode – Ag/AgCl (KCl sat.).

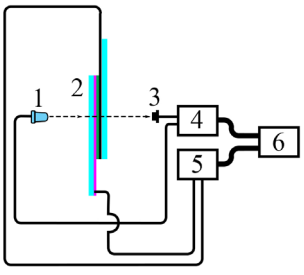

Fig. 3. Simplified schematic of the setup used to study the characteristics of the electrochromic device: 1 — source of white light (5,500 K); 2 — assembled electrochromic device; 3 — photoresistor; 4 — ADC; 5 — digital potentiostat; 6 — computer

5. Analysis and comparison of recorded characteristics of the electrochromic device with the mesh electrode

The electrodes of the electrochromic device operate in counter-phase, according to equations (1) and (2):

$$Ni(OH)_2 \rightarrow NiOOH + H^+ \text{ (electrochromic electrode)}, \quad (1)$$

trans.→brown,

$$Ag_XO_Y + Y \cdot H_2O \rightarrow X \cdot Ag + 2Y \cdot OH^- \text{ (mesh electrode)}, \quad (2)$$

Because of that, a layer of silver oxides had to be formed before assembly. The oxide layer was formed by means of cyclic voltammetry into positive potentials (Fig. 4). At potentials above +400 mV, the mesh electrode changed color from shiny silver grey to matte black. Obviously, this corresponds to the oxidation of Ag° to Ag_2O and Ag_2O to AgO. During cycling, this electrode demonstrated high electrochemical activity – a few high peaks were observed on the cyclic voltammetry (CV) curve, which were growing during cycling. This is likely related to the development of surface silver layer during cycling.

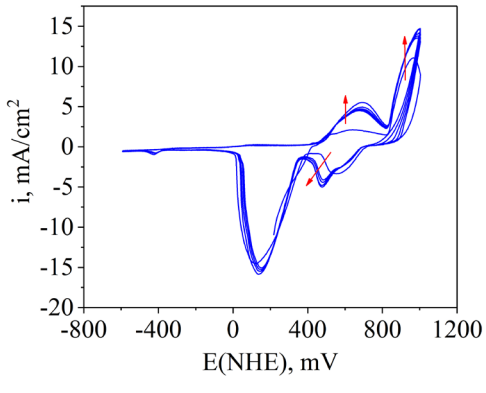

Fig. 4. CV curve of silver-coated wire in 0.1 M KOH (arrows indicate changes during cycling)

Fig. 5 shows glass after soft electrochemical etching with deposited electrochrome (deposition height 2 cm). As can be seen from the presented photographs, the quality of the prepared electrode is rather high. A few of such electrodes were used to determine the working current density from their CV curves and assembly the finished electrochromic device.

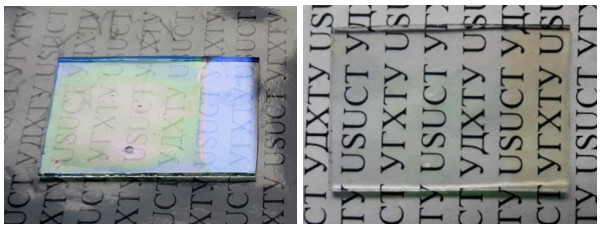

a *b*

Fig. 5. Photographs of FTO electrode with deposited electrochromic films that was previously subjected to soft electrochemical etching: *a* — in reflected light; *b* — perpendicular to the surface

In [24], it is shown that the electrochromic properties of nickel hydroxide-based electrodes show the best characteristics in the galvanostatic regimes. Thus, it was decided to conduct the first test of the assembled device in the galvanostatic regime. In order to choose the cycling current, a separate electrode was made, according to stages 1–3 (Fig. 2). The electrode was studied by means of cyclic voltammetry. Cycling results are shown in Fig. 6.

The obtained CV curve characterizes the electrode as reversible – starting from the second cycle, the peak shape and height remain almost constant. Half the height of the cathodic peak was then chosen as the working current density, which is equal to about 0.25 mA/cm^2. Given that the working area of the electrochromic electrode is 2×2=4 cm^2, the cycling current for the electrochromic device was 1 mA. Coloration and bleaching of the assembled device were realized by switching the polarity of the working current.

Fig. 7 shows the initial voltage curves of the electrochromic device during coloration-bleaching. Analysis of the curve shape indicated that some development of active material occurs. This is evident from changes in the curve shape for the coloration process, which is expressed as the elevation at the end. In turn, for the bleaching process, a significant increase in voltage from cycle to cycle at the initial moment is observed, along with elongation of the horizontal plateau. It should be noted that the visual analysis of video recording at the start of device's operation allows stating that a small coloration initially occurs near the wire of the mesh electrode. The color then propagates away from the wire, leaving partly colored areas in the middle of the electrode. Based on this finding, it can be said that in factory setting, the device would require preliminary cycling of several dozen cycles after assembly before delivery to users.

Fig. 8 shows the coloration-bleaching curves of the first seven cycles of galvanostatic cycling. The increase in coloration depth (difference between the colored and bleached states) during cycling indicates the initial development of active materials.

Further cycling of the device revealed the increase of coloration degree to 80 % – Fig. 9. Starting from cycle 30, the optical characteristics stabilized and were almost constant. Coloration and bleaching occurred almost linearly in time – Fig. 9, *b*.

The curve voltage continued to change – Fig. 10. This is likely due to the development of the silver electrode, as the optical characteristics of $Ni(OH)_2$ electrode stabilized.

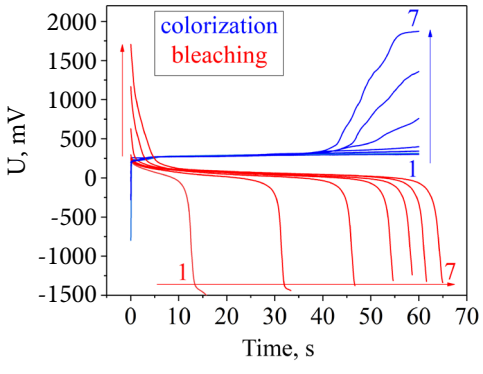

Fig. 7. Voltage change on the electrochromic device during galvanostatic cycling: +/−1 mA (arrows indicate the increase of the cycle number during coloration and bleaching, numbers — cycle numbers corresponding to the curves)

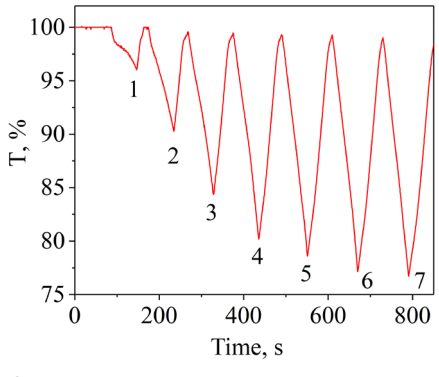

Fig. 8. Coloration-bleaching curve of the electrochromic device during galvanostatic cycling: +/−1 mA (1–7 cycle)

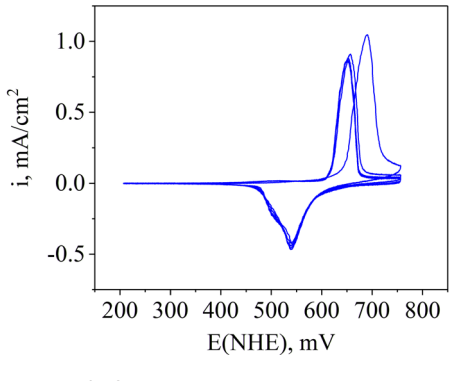

Fig. 6. CV curve of the electrochromic electrode $(Ni(OH)_2/PVA)$* in 0.1 M KOH at 1 mV/s (*substrate — FTO glass after soft electrochemical etching)

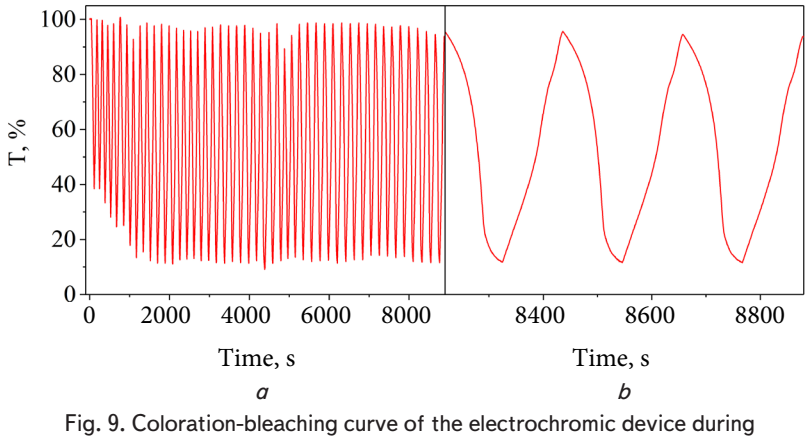

a *b*

Fig. 9. Coloration-bleaching curve of the electrochromic device during galvanostatic cycling: +/−1 mA (cycle 20–70): *a* — general view of coloration-bleaching curve (left); *b* — cycles 68–70 of coloration-bleaching (right)

As it was assumed that coloration and bleaching occur non-uniformly and start from the mesh electrode (Fig. 11). It is also interesting that with the development of materials, the non-uniformity of coloration became less pronounced.

Despite the non-uniform occurrence of the coloration-bleaching process, it is possible to achieve uniform coloration for such design of the device. Thus, after the current polarity was switched during the start of the bleaching process (5–10 s), the edges are bleached to transparency of the central part.

After testing in the galvanostatic regime, it was decided to conduct tests in the voltodynamic regime. The following program was used:

– linear sweep from 0 to +1,500 mV, at 50 mV/s;

– 20 s at +1,500 mV;

– linear sweep from +1,500 to –1,200 mV, at 50 mV/s;

– 20 s at –1,200 mV.

As a result, a coloration-bleaching curve was obtained, which is shown in Fig. 12. Analysis of the dependency revealed that in such regime, the coloration degree lowered, and it did not beach completely (T=90 %). The shape of the curve stopped being linear, Fig. 12.

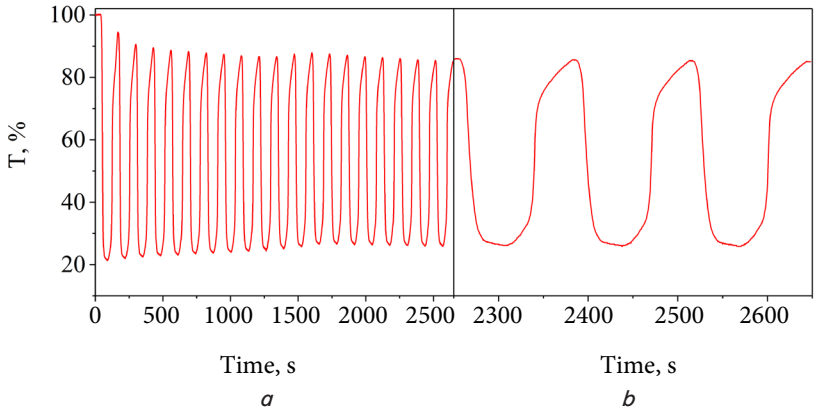

Fig. 12. Coloration-bleaching curve during voltodynamic cycling (20 cycles after 70 cycles of galvanostatic cycling): *a* – general view of the coloration-bleaching curve (left); *b* – 17–20 cycles of the coloration-bleaching curve (right)

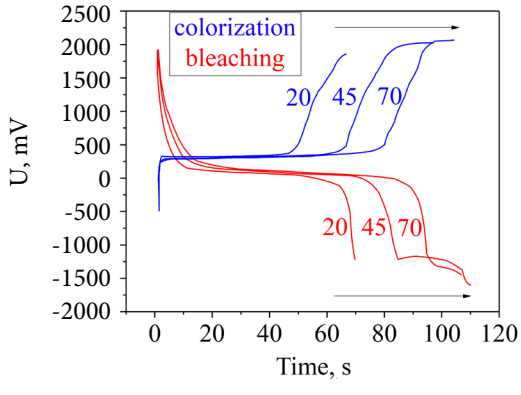

Fig. 10. Voltage at the electrochromic device during galvanostatic cycling: +/–1 mA (arrows indicate the increase of the cycle number during coloration and bleaching, numbers – cycle numbers corresponding to the curves)

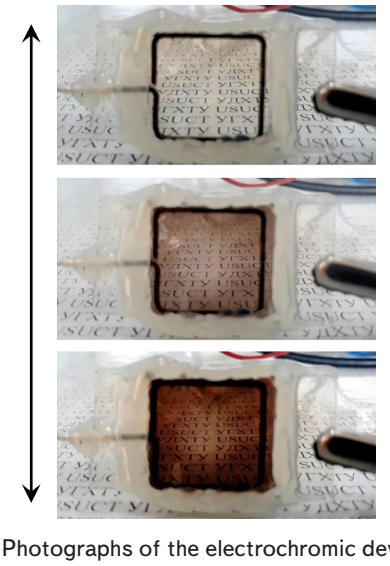

Fig. 11. Photographs of the electrochromic device with different degrees of coloration in the galvanostatic regime: +/–1 mA

Analysis of current consumption on the set voltage revealed voltages at which current consumption is maximum (Fig. 13). For the coloration process – 493 mV, for bleaching –38 mV.

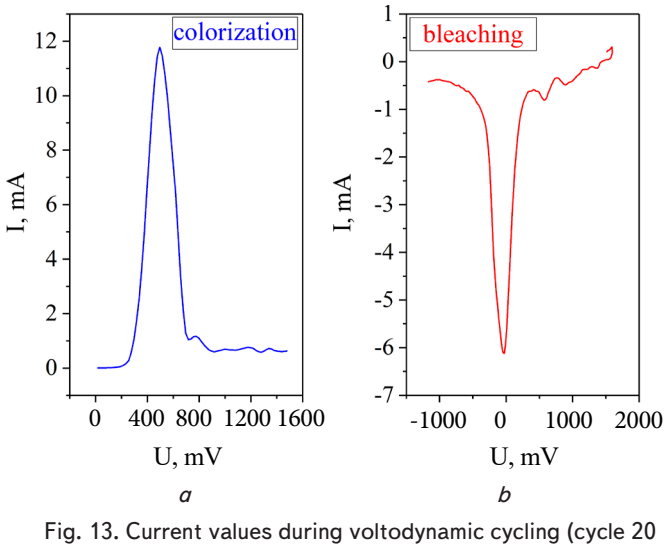

Fig. 13. Current values during voltodynamic cycling (cycle 20 after 70 cycles of galvanostatic cycling): *a* – coloration; *b* – bleaching

It should be noted that during all cycling experiments, no gas evolution was observed (i. e. electrolyte decomposition) [31]. This indicated that materials and cycling parameters were chosen correctly.

6. Discussion of obtained data for studied device

As a result of the study on the electrochromic device with the square wire electrode as a model of one cell of the mesh electrode, the possibility of operation of the electrochromic device with the mesh electrode is shown. After 90 cycles of coloration-bleaching in two cycling regimes, no gas evolution was observed. Bleaching and coloration

times did not exceed 2 min. It should be noted that for commercial electrochromic devices, typical switching time is 8–20 min [27, 28].

Coloration degree during galvanostatic cycling was 80 % and coloration was occurring unevenly. The unevenness is caused by electrolyte resistance [29, 30]. Lower resistance between the mesh electrode and the nearest zone of the electrochromic electrode is more favorable for the occurrence of the coloration process in this zone. After partial coloration in zones near the metal, the process starts to propagate. It is likely that with the increase of electrolyte conductivity, this effect can be partially removed. This assumption is supported by the CV curve of the electrochromic electrolyte with free electrolyte, where the distance between the electrodes is equal (Fig. 6). The stationary state is achieved at the third cycle, after which the shape of the curve is static. Despite the uneven coloration, it can be partially alleviated by short-term polarity reversal. Such idea occurred during the analysis of video recording of the bleaching-coloration process.

The coloration-bleaching curve during galvanostatic cycling has an almost linear form, which is a good operational characteristic. This indicates that coloration degree can be gradually controlled.

It should also be noted that after cycle 30, the characteristics of the electrochromic device during galvanostatic cycling were almost constant.

The voltodynamic regime, which was proposed based on the characteristics obtained from galvanostatic cycling (Fig. 10), turned out to be worse. The film did not bleach completely. Coloration degree was somewhat lower and the shape of the coloration-bleaching curve was not linear. Additionally, voltages were found at which the maximum current consumption was observed, which are +493 and −37 mV for coloration and bleaching, respectively. Perhaps, better operation of the electrochromic device can be achieved by correcting the voltodynamic regime based on the obtained data.

It is interesting to note that due to a small difference between the working potentials of the working electrode, the polarity of the working voltage during coloration and bleaching changes Fig. 7, 10.

Over the course of this study, the limit voltage values were found, above which decomposition of the electrolyte along with gas evolution would occur. Thus, the voltage limits are about +2,050 and −1,600 mV. A regime was found at which coloration of the device occurs linearly and reversibly -0.25 mA/cm^2.

It should be noted that the continuation of this study can be investigation of optimal operation parameters of the electrochromic device. For instance, investigation of optimal geometrical parameters (distance between electrodes, size and shape of the mesh electrode, etc.); use of thickened electrolyte and different KOH concentrations can be the next steps.

7. Conclusions

1. The possibility for developing full-size electrochromic devices for upper parts of view windows and light windows was demonstrated using a laboratory-scale prototype assembled using silver mesh electrode and electrochromic electrode based on $Ni(OH)_2$/PVA composite. It was also found that the coloration of the electrochromic device occurs with a small gradient, which can be removed with an impulse of reverse polarity currents.

2. The working parameters were found for the proposed electrochromic device: working current density 0.25 mA/cm^2 and voltage window from +2,050 to −1,600 mV.

References

1. Lim, C., Kim, K.-J., Maglio, P. P. (2018). Smart cities with big data: Reference models, challenges, and considerations. Cities, 82, 86–99. doi: https://doi.org/10.1016/j.cities.2018.04.011
2. Casini, M. (2014). Smart windows for energy efficiency of buildings. Proc. of the Second Intl. Conf. on Advances in Civil, Structural and Environmental Engineering- ACSEE 2014, 273–281.
3. Smart Windows: Energy Efficiency with a View. Available at: https://www.nrel.gov/news/features/2010/1555.html
4. Al Dakheel, J., Tabet Aoul, K. (2017). Building Applications, Opportunities and Challenges of Active Shading Systems: A State-of-the-Art Review. Energies, 10 (10), 1672. doi: https://doi.org/10.3390/en10101672
5. Smart windows: electrochromic windows for building optimisation. Available at: https://www.sageglass.com/sites/default/files/masdar_technology_journal_issue_5_september_2018_smart_windows.pdf
6. Kraft, A. (2018). Electrochromism: a fascinating branch of electrochemistry. ChemTexts, 5 (1). doi: https://doi.org/10.1007/s40828-018-0076-x
7. Lee, E. S., DiBartolomeo, D. L., Selkowitz, S. E. (2000). Electrochromic windows for commercial buildings: Monitored results from a full-scale testbed. LBNL Publications, 1–16.
8. Cheng, W., Moreno-Gonzalez, M., Hu, K., Krzyszkowski, C., Dvorak, D. J., Weekes, D. M. et. al. (2018). Solution-Deposited Solid-State Electrochromic Windows. iScience, 10, 80–86. doi: https://doi.org/10.1016/j.isci.2018.11.014
9. Low cost voltage-controlled window can be tuned to block visible and/or infrared light. Available at: https://arpa-e.energy.gov/sites/default/files/documents/files/UTAustin_OPEN2012%20_ExternalProjectImpactSheet_FINAL.pdf
10. Alesanco, Y., Viñuales, A., Rodriguez, J., Tena-Zaera, R. (2018). All-in-one gel-based electrochromic devices: Strengths and recent developments. Materials, 11 (3), 414. doi: https://doi.org/10.3390/ma11030414
11. Pehlivan, İ. B., Marsal, R., Pehlivan, E., Runnerstrom, E. L., Milliron, D. J., Granqvist, C. G., Niklasson, G. A. (2014). Electrochromic devices with polymer electrolytes functionalized by SiO_2 and In_2O_3:Sn nanoparticles: Rapid coloring/bleaching dynamics and strong near-infrared absorption. Solar Energy Materials and Solar Cells, 126, 241–247. doi: https://doi.org/10.1016/j.solmat.2013.06.010

12. Atak, G., Coşkun, Ö. D. (2019). Effects of anodic layer thickness on overall performance of all-solid-state electrochromic device. Solid State Ionics, 341, 115045. doi: https://doi.org/10.1016/j.ssi.2019.115045
13. Yang, X., Cong, S., Li, J., Chen, J., Jin, F., Zhao, Z. (2019). An aramid nanofibers-based gel polymer electrolyte with high mechanical and heat endurance for all-solid-state NIR electrochromic devices. Solar Energy Materials and Solar Cells, 200, 109952. doi: https://doi.org/10.1016/j.solmat.2019.109952
14. Wu, T.-Y., Li, W.-B., Kuo, C.-W., Chou, C.-F., Liao, J.-W., Chen, H.-R., Tseng, C.-G. (2013). Study of poly(methyl methacrylate)-based gel electrolyte for electrochromic device. International Journal of Electrochemical Science, 8 (8), 10720–10732.
15. Sonavane, A. C., Inamdar, A. I., Deshmukh, H. P., Patil, P. S. (2010). Multicoloured electrochromic thin films of NiO/PANI. Journal of Physics D: Applied Physics, 43 (31), 315102. doi: https://doi.org/10.1088/0022-3727/43/31/315102
16. Kotok, V., Kovalenko, V. (2019). Material selection for the mesh electrode of electrochromic device based on $Ni(OH)_2$. Eastern-European Journal of Enterprise Technologies, 4 (6 (100)), 54–60. doi: https://doi.org/10.15587/1729-4061.2019.176439
17. Kotok, V. A., Kovalenko, V. L., Kovalenko, P. V., Solovov, V. A., Deabate, S., Mehdi, A. et. al. (2017). Advanced electrochromic Ni(OH)2/PVA films formed by electrochemical template synthesis. ARPN Journal of Engineering and Applied Sciences, 12 (13), 3962–3977.
18. Kotok, V., Kovalenko, V. (2017). The electrochemical cathodic template synthesis of nickel hydroxide thin films for electrochromic devices: role of temperature. Eastern-European Journal of Enterprise Technologies, 2 (11 (86)), 28–34. doi: https://doi.org/10.15587/1729-4061.2017.97371
19. Gayon Lombardo, A., Simon, B. A., Taiwo, O., Neethling, S. J., Brandon, N. P. (2019). A pore network model of porous electrodes in electrochemical devices. Journal of Energy Storage, 24, 100736. doi: https://doi.org/10.1016/j.est.2019.04.010
20. Ranmode, V., Bhattacharya, J. (2019). Macroscopic modelling of the discharge behaviour of sodium air flow battery. Journal of Energy Storage, 25, 100827. doi: https://doi.org/10.1016/j.est.2019.100827
21. Bar, G., Strum, G., Gvishi, R., Larina, N., Lokshin, V., Khodorkovsky, V. et. al. (2009). A new approach for design of organic electrochromic devices with inter-digitated electrode structure. Solar Energy Materials and Solar Cells, 93 (12), 2118–2124. doi: https://doi.org/10.1016/j.solmat.2009.08.013
22. Kotok, V., Kovalenko, V., Malyshev, V. (2017). Comparison of oxygen evolution parameters on different types of nickel hydroxide. Eastern-European Journal of Enterprise Technologies, 5 (12 (89)), 12–19. doi: https://doi.org/10.15587/1729-4061.2017.109770
23. Kotok, V. A., Kovalenko, V. L. (2019). Non-Metallic Films Electroplating on the Low-Conductivity Substrates: The Conscious Selection of Conditions Using $Ni(OH)_2$ Deposition as an Example. Journal of The Electrochemical Society, 166 (10), D395–D408. doi: https://doi.org/10.1149/2.0561910jes
24. Kotok, V. A., Malyshev, V. V., Solovov, V. A., Kovalenko, V. L. (2017). Soft Electrochemical Etching of FTO-Coated Glass for Use in $Ni(OH)_2$-Based Electrochromic Devices. ECS Journal of Solid State Science and Technology, 6 (12), P772–P777. doi: https://doi.org/10.1149/2.0071712jss
25. Kotok, V. A., Kovalenko, V. L., Zima, A. S., Kirillova, E. A. Burkov, A. A., Kobylinska, N. G. et. al. (2019). Optimization of electrolyte composition for the cathodic template deposition of $Ni(OH)_2$-based electrochromic films on FTO glass. ARPN Journal of Engineering and Applied Sciences, 14 (2), 344–353.
26. Kotok, V., Kovalenko, V. (2018). A study of the effect of cycling modes on the electrochromic properties of $Ni(OH)_2$ films. Eastern-European Journal of Enterprise Technologies, 6 (5 (96)), 62–69. doi: https://doi.org/10.15587/1729-4061.2018.150577
27. Cheng, W., He, J., Dettelbach, K. E., Johnson, N. J. J., Sherbo, R. S., Berlinguette, C. P. (2018). Photodeposited Amorphous Oxide Films for Electrochromic Windows. Chem, 4 (4), 821–832. doi: https://doi.org/10.1016/j.chempr.2017.12.030
28. Smart Films. Electrochromic glass. Available at: http://smartfilmsinternational.com/wp-content/uploads/solar/SFI-Electrochromic-brochure.pdf
29. Fleig, J., Maier, J. (1997). The Influence of Inhomogeneous Potential Distributions on the Electrolyte Resistance in Solid Oxide Fuel Cells. ECS Proceedings Volumes, 1997-40, 1374–1384. doi: https://doi.org/10.1149/199740.1374pv
30. Sangeetha, T., Chen, P.-T., Cheng, W.-F., Yan, W.-M., Huang, K. (2019). Optimization of the Electrolyte Parameters and Components in Zinc Particle Fuel Cells. Energies, 12 (6), 1090. doi: https://doi.org/10.3390/en12061090
31. Kotok, V. A., Kovalenko, V. L. (2019). A New Low-cost Semitransparent Electrochromic Device Based on $Ni(OH)_2$/FTO and Ag_XO_Y/Cu Electrodes. Electrochemistry Conference – 2019, 30. Available at: https://electrochem2019.meetinghand.com/projectData/869/webData/Elektro-2019-Book_k.pdf